

RESEARCH

Open Access



Association of spectroscopically determined leaf nutrition related traits and breeding selection in *Sassafras tzumu*

Jun Liu^{1†}, Yang Sun^{1,2†}, Wenjian Liu¹, Zifeng Tan¹, Jingmin Jiang¹ and Yanjie Li^{1*} 

Abstract

Background: Plant traits related to nutrition have an influential role in tree growth, tree production and nutrient cycling. Therefore, the breeding program should consider the genetics of the traits. However, the measurement methods could seriously affect the progress of breeding selection program. In this study, we tested the ability of spectroscopy to quantify the specific leaf nutrition traits including anthocyanins (ANTH), flavonoids (FLAV) and nitrogen balance index (NBI), and estimated the genetic variation of these leaf traits based on the spectroscopic predicted data. Fresh leaves of *Sassafras tzumu* were selected for spectral collection and ANTH, FLAV and NBI concentrations measurement by standard analytical methods. Partial least squares regression (PLSR), five spectra pre-processing methods, and four variable selection algorithms were conducted for the optimal model selection. Each trait model was simulated 200 times for error estimation.

Results: The standard normal variate (SNV) to the ANTH model and 1st derivatives to the FLAV and NBI models, combined with significant Multivariate Correlation (sMC) algorithm variable selection are finally regarded as the best performance models. The ANTH model produced the highest accuracy of prediction with a mean R^2 of 0.72 and mean RMSE of 0.10%, followed by FLAV and NBI model (mean R^2 of 0.58, mean RMSE of 0.11% and mean R^2 of 0.44, mean RMSE of 0.04%). High heritability was found for ANTH, FLAV and NBI with h^2 of 0.78, 0.58 and 0.61 respectively. It shows that it is beneficial and possible for breeding selection to the improvement of leaf nutrition traits.

Conclusions: Spectroscopy can successfully characterize the leaf nutrition traits in living tree leaves and the ability to simultaneous multiple plant traits provides a promising and high-throughput tool for the quick analysis of large size samples and serves for genetic breeding program.

Keywords: Spectroscopy, Anthocyanins (ANTH), Flavonoids (FLAV), Nitrogen balance index (NBI), breeding selection

Background

Nitrogen (N) is one of the most essential nutrients in plant growth, which is needed for the improvement of grain yield and quality [10]. Excessive N fertilizer application creates severe environmental problems, while

inadequate N availability limits productivity. Hence, precise N application in plant is an important goal [74]. The N status of the plant should be precisely measured during growth to guide precise fertilization [63]. N is the most common limiting factor for the individual, natural and artificial ecosystems growth of the plant. Plants require N to maintain for growth mainly through external and internal sources, including soil organic matter, fertilizers, atmospheric deposition and stored N by plant themselves [52]. Plants, such as boreal species, store N seasonally through the process of internal cycling and it is a major

*Correspondence: aj7105@gmail.com

[†]Jun Liu and Yang Sun contributed equally to this work

¹Research Institute of Subtropical Forestry, Chinese Academy of Forestry, Fuyang 311400, Zhejiang, China

Full list of author information is available at the end of the article



source of N supplement for tree growth especially when the external availability of N is limited [54, 59]. Trees store N as proteins mainly in their perennial wood and bark tissues in summer and winter. In addition, other parts of foliage trees, like roots and leaves, also store N which provides nutrition for young roots and needles development. Tree N remobilisation often occurs during the growth season. The stored N mainly determines the amount of N remobilised and plays an important role for the tree seasonal growth [2, 11, 82]. The dynamics and mobilization of N stored in trees have been widely studied [15, 45]. The variation of plant species, genotype, soil and environment leads to the diversity of leaf nitrogen content [20, 73]. It is reported that the chlorophyll content has a strong positive correlation with N content which is an estimative index for N status in leaf [87]. Chlorophyll content is measured as a proxy for leaf N status [19] and non-destructive, spectroscopic, chlorophyll meters have been available for decades [19, 31, 33, 48, 56, 57]. In addition to chlorophyll, the content of flavonoids (FLAV), one of the main polyphenolic components in plant, is also correlated with the N status of the leaf [80]. Evidence shows that the rise of N fertilization will lead to flavonoid content decreasing and chlorophyll content increasing [60]. Another N status index, N balance index (NBI), which is the ratio of chlorophyll to flavonoid, is verified that has a better and more reliable correlation with leaf N concentration than chlorophyll content alone [80].

Anthocyanins (ANTH) are a group of water soluble flavonoid pigments that occur in all plant tissues. Anthocyanins are mostly related to a wide range of plant colour but often appear as red [13]. In addition, unfavourable conditions will transiently have an impact on anthocyanins accumulation in both juvenile and senescent observable plant leaves [25, 58, 81]. Thus, Anthocyanins are taken as an indicator of plant leaf senescence and stresses [44, 62].

However, research on plant growth and the variation of N storage and remobilization have typically required labour intensive methods to measure the N concentration and index properties (NBI, ANTH, and FLAV), such as atomic absorption spectrometry [8, 32], chromatography [68] and so on. These analytical methods will limit the breeding selection of tree growth with a large number of samples.

Alternatively, Near-infrared spectroscopy (NIRS) is a rapid, high-throughput technique that has been used for chemical components analysis in many fields. NIRS is a promising and reliable method that can be used for the assessment of a large number of samples [23, 27, 40, 46, 67]. NIRS relies on the absorption of light at specific wavelengths due to the vibration, stretching and bending

of molecular bonds, including C–H, N–H and O–H bonds [6, 72].

Multivariate methods such as partial least squares regression (PLSR) [86] has been used to create a prediction model between NIR spectra and the independent chemical measurements. PLSR holds the advantages of producing reliable coefficients, reducing the bias and estimated error, and consuming fewer PLSR components, all of which make it one of the most popular methods for chemometric analyses [1, 7]. The model will then be applied to unknown samples by their spectra data for independent chemical prediction. Our recent research shows that leaf chlorophyll content and colour parameters are predictable on fresh leaf samples with field near infrared spectrophotometry [41]. The total FLAV and ANTH concentration also have been predicted by a general calibration model in *Ginkgo biloba* leaf and four Indonesian herbal plant species, including *Syzygium oleana*, *Piper betle*, *Jasminum* and *Graptophyllum pictum* with NIR reflectance spectroscopy. NIR is a promising tool for tree breeding selection programs due to its robustness and capacity to screen large numbers of samples [26, 41].

The robustness and reliability of model accuracy are largely determined by the spectra quality and feature selection. The combinations vibrations information and noise of the raw NIR spectra [89] will result in overlapping and difficulty to directly distinguish the target plant properties [34]. Spectra pre-processing methods, can efficiently reduce the overlapping and noise influence, such as SNV [3], 1st and 2nd derivatives and so on [36, 61]. To yield a robust and reliable model and avoid the influence of irrelevant variables and noise, it is essential to carry out variable selection methods to pick the most relevant variables responding to the target properties instead of the full length of spectra [21, 43].

The joint analyses of chemometric statistics and variable selection algorithms has recently been used to eliminate the irrelevant variables and improve the model accuracy [9, 47]. The most common methods of variable selection are Genetic algorithm (Ga) [91], Regularized elimination procedure (Rep) algorithm [49], Iterative predictor weighting (Ipw) [22] and significant Multivariate Correlation (sMC) algorithm [79]. However, the comparison of variable selection algorithms along with PLSR for the prediction of multiple leaf nutrition traits is less studied.

Sassafras tzumu is a deciduous tree species that has colourful leaves in autumn. Zhejiang province in China is vigorously promoting the cultivation of colourful species making *S. tzumu* a famous tree species. It has been widely planted in Zhejiang province to develop the urban and mountain landscape [35].

Therefore, the aims of this research are to (1) test the capacity of reflectance spectroscopy to characterize the NBI, ANTH and FLAV with PLSR model; (2) find out the most optimal pre-processing method for these three leaf traits. (3) Identify the most important wavelength that related to NBI, ANTH and FLAV by four variable selection methods, including significant multivariate correlation (sMC), regularized variable elimination procedure (Rep), iterative predictor weighting (Ipw), and Genetic algorithm (Ga) variable selection; (4) estimate genetic parameters and correlations of NBI, ANTH and FLAV in *S. tsumu*.

Methods and materials

Materials

50 half-sib families of *S. tsumu* were selected for our study from 6 different regions. Trees were planted in 2016 using a randomised complete block by a 2 m × 3 m spacing in Changle Forest Farm Nursery (30° 27' N, 119° 48' E), Hangzhou, Zhejiang, China. Each family replicated 30 times with 5 replications and 6 individual trees per replication. In total, 1500 trees were planted.

NIR spectra collection

Samples spectra data was collected through 5–6 leaves of each tree from the top to bottom with similar color on the same side in October 2018. The NIR spectra data was taken from the upside surface of the leaves three times with a handheld fibre optic contact probe from a field-based spectrometer (LF-2500, Spectral evolution, USA). Each spectrum took on average 32 scans with a range of 1100 to 2500 nm by a 6 nm resolution. All spectra were obtained from the leaves of 1500 trees, 500 trees leaves from these 1500 trees were sampled and placed in a marked paper bag and transferred to the refrigerator immediately for chemical measurement.

Leaf FLAV measurement

Each leaf was ground into powder and being mixed with methanol for 24 h. 0.5 ml (1 mg/ml) extract of each sample was taken to mixed with methanol (1.5 ml), 10% aluminium chloride (0.1 ml), 1 M potassium acetate (0.1 ml) and distilled water (2.8 ml). The mixture was being placed under room temperature for 30 min and then measured at 415 nm for the absorbance by UV–Visible spectrophotometer (UV-1280, Shimadzu, Japan). The flavonoid content of the sample was accessed by the value of absorbance density [18].

Pigment extraction and NBI estimation

A weighed circular piece cutting from each leaf was placed into a mortar by a pestle ground with 100% methanol until the colour changed into white. The extract was being centrifuged for 6 min by 14,000 rpm at 4 °C and subsequently assayed by a UV–Visible spectrophotometer (UV-1280, Shimadzu, Japan). It conducted the equation and specific absorption in the wavelength which was reported by Wellburn [83]. The solution was mixed with 3 ml acidified methanol (1% HCl) at 4 °C with moderate shaking for 12 h and then being centrifuged for 10 min at 14,000 rpm. The extraction was then placed into the spectrophotometer, it took the absorption at 530 and 657 nm wavelengths to determine the ANTH concentration [76]. The NBI index was figured as the ratio of chlorophyll to flavonoid content.

Model calibration and validation

The original five different types of pre-processing spectra (SNV, 1st, 2nd derivatives, SNV+1st derivatives, SNV+2nd derivatives) combined with PLSR [86] algorithm were compared in our study. The Savitzky–Golay smoothing [64] with a window size of 15 data points was applied in both 1st and 2nd derivatives spectra. PLSR models were generated with leave-one-out cross-validation for the prediction of ANTH, NBI, and FLAV content. Data were randomly split 200 times into calibration (80%) for model building and validation (20%) for model test respectively. Therefore, the PLSR model has been conducted 200 times for the evaluation of model performance. Each model combined with four variable selections (sMC, Ipw, Rep and Ga) was conducted to find out the most important spectral variables. The coefficient of determination (R^2) and root-mean-square error (RMSE) in each model derived from both calibration (Cal) and validation (Val) were applied for the evaluation model performance.

Statistical analysis

The estimation of genetic parameters were measured by a multivariate restricted maximum likelihood (REML) linear mixed model, details can be found in Li et al. [40]. The narrow sense heritability (h^2) of trait i and genetic correlations (r_{gij}) and phenotypic correlation ($r_{p_{ij}}$) between trait i and trait j were calculated as:

$$h_i^2 = \frac{2.5\sigma_{f_i}^2}{\sigma_{f_i}^2 + \sigma_{e_i}^2}$$

$$r_{gij} = \frac{\sigma_{f_{ij}}}{\sqrt{\sigma_{f_i}^2 + \sigma_{f_j}^2}}$$

$$r_{p_{ij}} = \frac{\sigma_{f_{ij}} + \sigma_{e_{ij}}}{\sqrt{(\sigma_{f_i}^2 + \sigma_{e_i}^2)(\sigma_{f_j}^2 + \sigma_{e_j}^2)}}$$

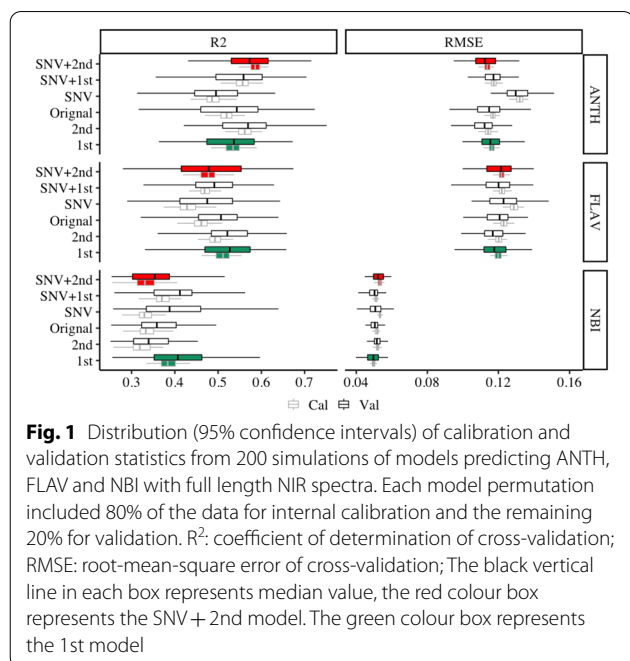
where $\sigma_{f_i}^2$ is the estimated family variance for trait i , and $\sigma_{f_j}^2$ is the estimated family variance for trait j , $\sigma_{e_i}^2$ and $\sigma_{e_j}^2$ are the residual variances for trait i and j , and $\sigma_{f_{ij}}$ and $\sigma_{e_{ij}}$ are the family and residual covariances between traits i and trait j . The random effects of each family were set as breeding values. The realized genetic gain (ΔG_R) was calculated by the difference between the mean breeding values of selected top ratio leaf traits and the total mean of the leaf traits.

R software (version 3.1.2) [66] was used for all of the data analysis. The *pls* package [50] in R was carried out for PLSR model building, and the *plsVarSel* [49] for variables selection, the *prospectr* package [75] for NIR spectra manipulation, the *lme4* package [4] for estimation of genetic parameters, and the *ggplot2* package [84] for visualization plot.

Results

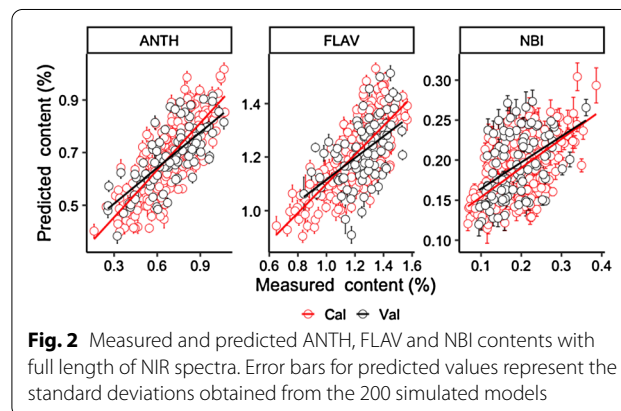
Model performance

Figure 1 displays the NIR spectral PLSR model for ANTH, FLAV and NBI traits. ANTH model has the highest accuracy, followed by FLAV and NBI model. The average of R^2 and RMSE for these three models in calibration (Cal) sets are 0.54 (range: 0.43–0.63), 0.47 (range: 0.35–0.58) and 0.36 (range: 0.26–0.45), in validation (Val) sets are 0.54 (range: 0.28–0.75), 0.47 (range: 0.28–0.69)



and 0.38 (range: 0.25–0.64) respectively. As for all spectral pre-processing models, SNV + 2nd derivative prediction model is found to be the highest well-performing for predicting ANTH concentration than the other pre-processing methods, with a mean R^2_{Cal} and $RMSE_{Cal}$ of 0.59 (range: 0.55–0.63), 0.11% (range: 0.11–0.12%), a mean R^2_{Val} and $RMSE_{Val}$ of 0.57 (range: 0.38–0.72), 0.11% (range: 0.09–0.13%), followed by 2nd, SNV + 1st, 1st, original with the mean of R^2 in Cal is 0.56 (range: 0.42–0.75), 0.56 (range: 0.51–0.60), 0.53 (range: 0.48–0.59), 0.52 (range: 0.47–0.56), and $RMSE$ 0.11% (range: 0.11–0.12%), 0.11% (range: 0.11–0.12%), 0.11% (range: 0.11–0.12%), 0.12% (range: 0.11–0.12), and in Val is 0.57 (range: 0.42–0.75), 0.54 (range: 0.30–0.70), 0.53 (range: 0.36–0.67), 0.52 (range: 0.32–0.72), and $RMSE$ 0.11% (range: 0.09–0.13%), 0.12% (range: 0.10–0.14%), 0.12% (range: 0.10–0.14%), 0.11% (range: 0.09–0.14%) respectively. SNV shows the worst effect with the mean of R^2 and $RMSE$ for Cal and Val 0.49 (range: 0.44–0.54), 0.49 (range: 0.28–0.63), and 0.13% (range: 0.13–0.14%), 0.13% (range: 0.12–0.16%) respectively. However, 1st yields the best PLSR model in the prediction of FLAV and NBI than the other pre-processing model, with high mean R^2_{Cal} R^2_{Val} of 0.51 (range: 0.46–0.58), 0.52 (range: 0.29–0.68), and low mean of $RMSE_{Cal}$, $RMSE_{Val}$ of 0.12% (range: 0.11–0.13%), 0.12 (range: 0.10–0.12%) in FLAV model and high mean R^2_{Cal} , R^2_{Val} of 0.39 (range: 0.33–0.45), 0.41 (range: 0.26–0.60), and low mean of $RMSE_{Cal}$, $RMSE_{Val}$ of 0.05% (range: 0.05–0.05%), 0.05 (range: 0.04–0.06%) in NBI model respectively. The effect of SNV shows a poor prediction in the FLAV and NBI as well. The mean of R^2_{Val} is 0.40 (range: 0.26–0.64) and 0.47 (range: 0.29–0.64) respectively.

The relationship between the predicted and measured content of Cal and Val datasets by ANTH model with SNV + 2nd derivative spectra, FLAV and NBI model with 1st derivative spectra were plotted in Fig. 2. The error bar represents the prediction error of 200 times per sample.



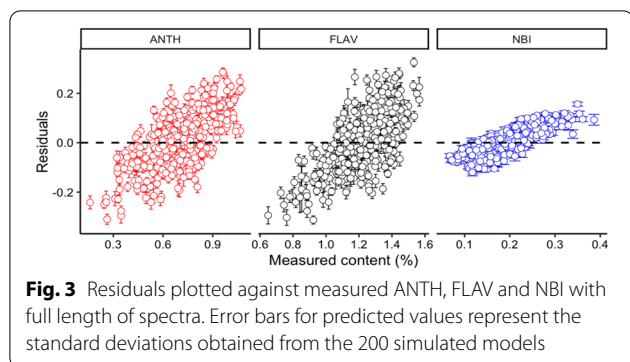


Fig. 3 Residuals plotted against measured ANTH, FLAV and NBI with full length of spectra. Error bars for predicted values represent the standard deviations obtained from the 200 simulated models

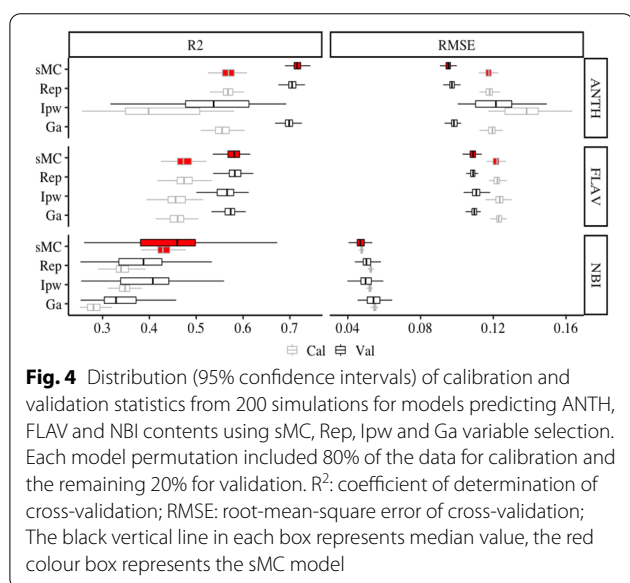


Fig. 4 Distribution (95% confidence intervals) of calibration and validation statistics from 200 simulations for models predicting ANTH, FLAV and NBI contents using sMC, Rep, Ipw and Ga variable selection. Each model permutation included 80% of the data for calibration and the remaining 20% for validation. R²: coefficient of determination of cross-validation; RMSE: root-mean-square error of cross-validation; The black vertical line in each box represents median value, the red colour box represents the sMC model

It shows that due to the high accuracy of the ANTH and FLAV models, the predicted values are more correlated with the measured values, while the relationship between predicted and measured values of NBI model is relatively poor. Although the prediction accuracy of each model is different, the prediction error of the Cal and Val data sets is still small.

The residual of the best processing spectra model for each leaf trait shows that all of these three models tend to be underpredicted when the measurement value is small. With the rise of the measurement value, the prediction value has the tendency of overprediction. The residual value of ANTH, FLAV and NBI model is between an acceptable range from -0.3 to 0.3 (Fig. 3).

Variable selection and model optimization

Four types of variable selection methods were compared to test the performance of ANTH, FLAV, and NBI PLSR models (Fig. 4). The prediction accuracy of ANTH, FLAV, and NBI PLSR models was enhanced much better than

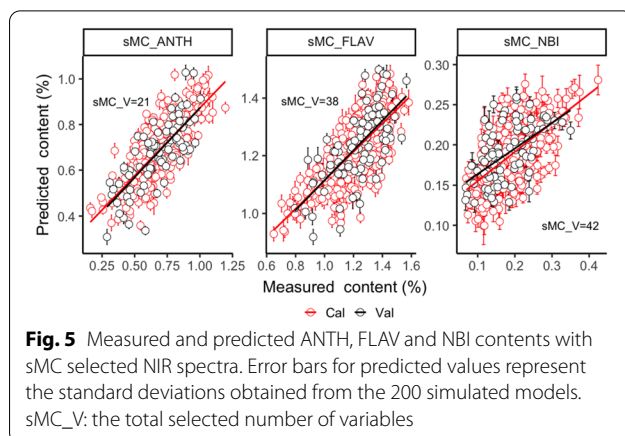


Fig. 5 Measured and predicted ANTH, FLAV and NBI contents with sMC selected NIR spectra. Error bars for predicted values represent the standard deviations obtained from the 200 simulated models. sMC_V: the total selected number of variables

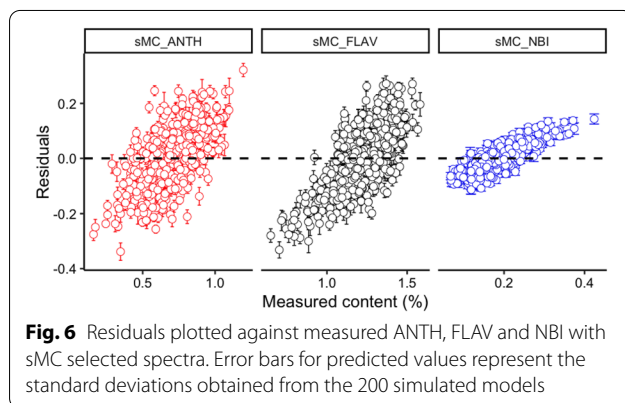


Fig. 6 Residuals plotted against measured ANTH, FLAV and NBI with sMC selected spectra. Error bars for predicted values represent the standard deviations obtained from the 200 simulated models

the full-length spectra models by these four different variable selection methods. ANTH model still holds the highest R² and RMSE value in both Cal and Val data, followed by the FLAV and NBI model. The highest prediction model for ANTH, FLAV and NBI was found through sMC-selected NIR spectra variables with the mean R²_{Val} of 0.72 (ranged: 0.69 to 0.75), 0.58 (ranged from: 0.54 to 0.62), 0.44 (ranged from: 0.26 to 0.67), and the mean RMSE_{Val} of 0.10% (range: 0.09–0.10%), 0.11% (range: 0.10–0.12%), 0.04% (range: 0.04–0.05%) respectively. The sMC_PLSR models reached a more stable prediction with less than 16% of full length of spectra on each leaf trait (Fig. 5), and having a similar residual range to the model with full length of spectra (Figure 6).

Figure 7 displays the important variable information area selected by sMC variable selection method in the ANTH, FLAV and NBI model which conducted 200 times on each model. Even the predicted model of three leaf traits was being run 200 times, sMC variable selection brought out stability for the selected important variable areas with a few relative spectral regions in prediction models. The variables at 2060, 2180, 2270, 2330 and 2440 nm are considered as the vital roles in the

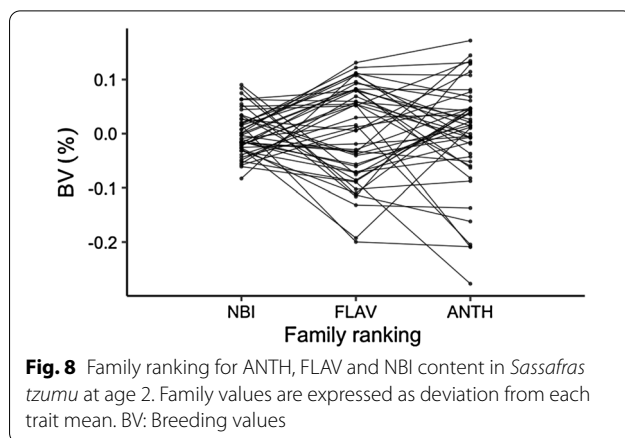
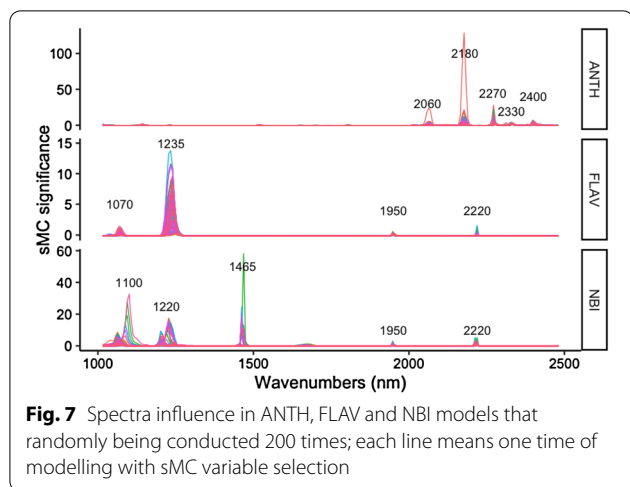


Table 1 The heritability, genetic (above diagonal (*italic*)) and phenotypic correlation (below diagonal) between ANTH, FLAV and NBI traits with the standard error between parentheses

Traits	ANTH	FLAV	NBI	<i>h</i> ²
ANTH		<i>0.36 (0.01)</i>	<i>0.11 (0.02)</i>	0.78 (0.10)
FLAV	0.16 (0.03)		<i>0.09 (0.01)</i>	0.58 (0.11)
NBI	0.09 (0.01)	0.12 (0.01)		0.61 (0.08)

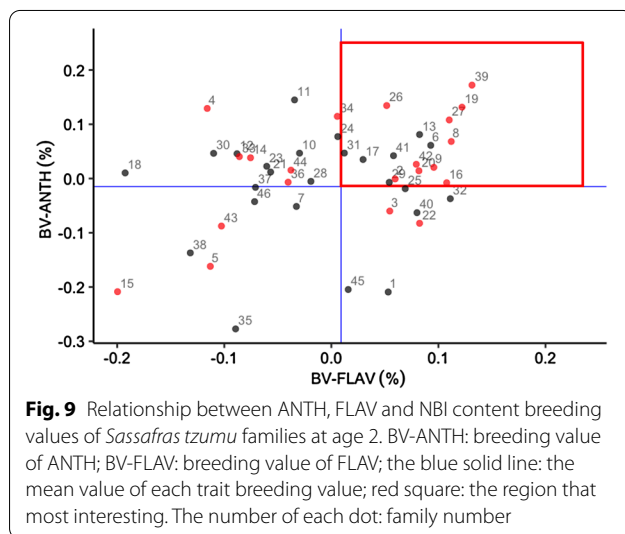
construction of ANTH prediction model. As for FLAV, 1070, 1235, 1950 and 2220 nm are the most important areas. Spectroscopic variables at 1100, 1220, 1465, 1950 and 2220 nm make a critical difference in the NBI predictive model.

Heritability, genetic and phenotypic correlation among traits

Table 1 shows the correlation (genetic and phenotypic) and heritability of three traits. Leaf ANTH produces the highest heritability of 0.78, followed by FLAV and NBI with *h*² of 0.58 and 0.61 respectively. There has no significant genetic and phenotypic correlation between ANTH, FLAV and NBI. FLAV was found to have the highest positive genetic correlation with ANTH with a value of 0.36.

Family selection

The best models of ANTH, FLAV and NBI were applied to predict the remaining 1000 trees spectra. In total, 1500 trees of 50 families were selected for breeding analysis. Figure 8 shows the distribution of three leaf traits in the ranking of breeding value from 50 families. The ranking of three leaf traits in different families is inconsistent as well as a part of families consistently displaying in the breeding value, which explains that it is feasible to make



a family selection of ANTH, FLAV and NBI at the same time through genetic selections.

Figure 9 demonstrates the breeding value distribution of 50 families of three leaf traits. The blue solid lines represent the average of ANTH and FLAV respectively. The families with a higher NBI breeding value than its mean are shown in red, and below the mean are in black. There are 16 families have high FLAV and ANTH breeding value, 10 families with a high breeding value will be selected If NBI breeding values are required to be above mean. These families can be further taken as genetic family materials for second-generation breeding.

Discussion

The health of tree growth is dictated by main factors, such as soil, nutrients, environment, genetic and so on. N is a key role of nutrient which highly influences the tree growth.

The internal N cycling in trees [78] is a hot topic in numerous studies [24, 38, 53]. However, the measurement of N concentration limits the access to the further study. In this study, the field-base reflectance spectroscopy has been proved to be a useful method to characterize the plant nutrition properties in fresh leaves. The SNV + 2nd derivative spectra for ANTH, and 1st derivative spectra for FLAV and NBI have been identified to increase the model accuracy when calibrating the PLSR prediction models. Incorporate with spectra variable selection, the model accuracy has been significantly improved with less variables for the prediction of leaf nutrition traits. Our model offered a reliable result for predicting the FLAV content in fresh leaf ($R^2_{\text{Val}}=0.58$, ranged from: 0.54 to 0.62), which was lower than the result reported for *fresh Ginkgo biloba* leaf in different colors ($R^2_{\text{CAL}}=0.82$ and $\text{RMSE}=2.62\%$) [71]. The variability lessened by small range of NBI value lead to an inefficient prediction [5].

Conversely, our prediction of ANTH content result illustrates a suitable accuracy than the other two leaf traits, with a mean R^2_{Val} of 0.72 (range: 0.69–0.75) and a mean of RMSE_{Val} of 0.09% (range: 0.09–0.10%). Similar result was discovered in wine grapes by NIR hyperspectral imaging and PLSR model, which gave R^2 of 0.84 and RMSEP of 0.013% for estimating ANTH content.

A robust statistical methodology for model calibration, which was first conducted by Couture et al. [12] to predict plant leaf secondary metabolites with reflectance spectroscopy, was applied in our study. It has being run 200 randomized simulations for calibrating the models to provide an estimation of the model uncertainty and overall stability (Figs. 1, 2, 3, 4, 5, 6, 7). It is similar to our previous study which takes use of filed spectroscopy to predict the leaf colour and chlorophyll content [41]. Random sampling [65] and Kennard-Stone sampling algorithm [42] in other studies, which sample only once for model calibration, may cause instability for model prediction. Thus, we highly recommend using this methodology for model calibration and validation on NIR analysis.

The NIR spectra involves not only the favourable information but noise and irrelevant information which will encumbrance the accuracy of prediction model. Therefore, variable selection is regarded as an efficient way to find out the most important wavelengths which contributes the minimum error for model calibration and helps to reduce the model processing time for spectral models. Variables in the spectrum play a key role in the predictive accuracy of the model. The spectral information is extensive along with the relevant and irrelevant information, both of which will overlap to interfere the model construction of the useful information and the PLSR model with a specific trait [88]. Thus, it is vital to

screen important variables for spectral information. In this study, four variable selection methods were compared to pick the best variable selection method. It shows that the sMC-PLSR model efficiently identified the key wavelengths and enables us to select a small set of variables to yield a promising and robust calibrated model for the prediction of ANTH, FLAV and NBI. Our results support the research announced by Li and Altaner [39], who successfully took the sMC variable selection method to improve the accuracy of an NIR calibration model on the prediction of extractives contents in heartwood of *Eucalyptus bosistoana* trees, and Li et al. [41] who found that sMC selection algorithm held the advantage of finding the most relevant variables for the prediction of leaf chlorophyll content and colour parameters. Some studies also states that significance multivariate correlation (sMC) [79] is a positive algorithm to remove confounding effects from NIR calibrations [85].

Several important variables which are related to the ANTH, FLAV, and NBI have been selected similarly in each model, including the range at 2060, 2180, 2270, 2330 and 2440 nm for ANTH, 1070, 1235, 1950, 2220 nm for FLAV, and 1100, 1220, 1465, 1950, 2220 nm for NBI respectively. As reported by Ramirez et al. [67], the regions around 2060, 2180, 2270, 2330 and 2440 nm are mostly associated with O–H and C–H stretching vibrations as well as the starch and sugar [17]. However, in our study, these regions have been ignored. The regions around 1070, 1100, 1220, 1235 nm are mainly assigned to the 1st overtones of C–H combination bands and 1st and 2nd overtones of O–H and N–H stretching vibrations, while the bands around 1465 nm are mostly related to the 1st overtones of O–H stretching vibration, both of which are associated with starch and protein [14, 16, 37]. In NIR spectra, water has a wide absorbance region which is a major influence on the other chemical information because of spectra overlap. In our study, the band around 1950 nm related to the water has less contribution to the FLAV and NBI model and no influence on the ANTH model. It probably influences the accuracy of model for the prediction of FLAV and NBI. Correlational study was found by Min et al. [55], who stressed that the regions of 1910 and 1938 nm highly related to water might have a strong impact on the N concentration prediction.

Trees N internal cycling is considered as one of the major ecology factors for tree growth and is an augment for the tree uptake of soil N [51]. In addition, it also helps to understand numerous aspects of plant ecology, for instance, to evaluate the effect of the N storage and remobilization in different part tissues of trees in relation to current demands for growth [70], to find out the role of N on growth stress, the relationship with N deposition in forest [28, 29] and the relationship with dynamics

of carbon recourse in trees [30, 82]. Our fast and accurate measurement of N index, including ANTH, FLAV and NBI traits of trees with NIR spectroscopy provides an advanced way for the study of N internal cycling and allows to quickly measure large number of samples.

In this study, we continue to use the coefficients of 1/2.5 for the calculation of heritability of ANTH, FLAV and NBI traits based on our previous study to avoid the assembling of half-siblings and inbreeding effects [41]. The moderate heritability of ANTH, FLAV and NBI was found, with the value of h^2 ranging from 0.61 to 0.78. The leaf ANTH heritability of 0.78 in our study is similar to the result found by Yihu et al. [77] who figured out the anthocyanin content heritability ranging from 0.79 to 0.91 in leaves of chili pepper higher than 0.29 reported in the leaf of Aspen (*Populus tremula* L.) [69]. For FLAV, a significant high rang of heritability from 0.94 to 0.99 was reported in the leave of Ginkgo Trees [90] which was much higher than our study ($h^2=0.58$). It indicates that genetic control capacity is different between species even the same traits. Our study proved that there is also a potential for the selection of NBI traits in breeding programs even with less study on the estimation of NBI heritability.

The consistence of families ranking of ANTH, FLAV and NBI indicates that the selection for a good leaf nutrition tree is workable, and the selection of qualified nutrition plant is supposed to involve multiple traits, which will afford a stable inheritance.

Conclusion

In conclusion, NIR spectroscopy is potentially taken to estimate the nutrition related traits by fresh leaf. With the small prediction error, the tree breeding programs can be successfully achieved based on the relative prediction value. Our study provides an alternative way for the N index traits and open a door to the efficient analysis of the internal N cycling in trees. The pre-processing method and variable selection highly influence the performance of model prediction. Our study found that by using of 1st and SNV + 2nd derivative spectra processing method and sMC variable selection algorithm, the PLSR models have been highly improved. In addition, the repeated spectral statistical methodology that we applied provided an efficient way to deal with variation in calibration data and generate information on the response of plant nutrition traits with NIR spectra. NIR model serves as an efficient tool for the estimation of genetic parameters and breeding selection in high throughput way to improve the leaf traits quality.

Acknowledgements

Not applicable.

Authors' contributions

YL designed the study, conducted the experiment, analysed the data and wrote the manuscript. JL, YS, WL and ZT conducted lab experiments and modified the manuscript. JJ supervised the experiments at all stages and reviewed the manuscript. All authors read and approved the final manuscript.

Funding

This work was funded by the collection evaluation and breeding technology of *Sassafras tzumu* germplasm resources (201804) and Zhejiang Science and Technology Major Program on Agricultural (Forestry) New Variety Breeding (2016C02056-10).

Availability of data and materials

Not applicable.

Declarations

Ethics approval and consent to participate

Not applicable.

Consent for publication

Not applicable.

Competing interests

The authors declare that there is no conflict of interest.

Author details

¹ Research Institute of Subtropical Forestry, Chinese Academy of Forestry, Fuyang 311400, Zhejiang, China. ² College of Forestry, Nanjing Forestry University, Nanjing, People's Republic of China.

Received: 24 July 2020 Accepted: 19 March 2021

Published online: 31 March 2021

References

- Asner GP, et al. Spectroscopy of canopy chemicals in humid tropical forests. *Remote Sens Environ*. 2011;115:3587–98. <https://doi.org/10.1016/j.rse.2011.08.020>.
- Babst BA, Coleman GD. Seasonal nitrogen cycling in temperate trees: transport and regulatory mechanisms are key missing links. *Plant Sci*. 2018;270:268–77. <https://doi.org/10.1016/j.plantsci.2018.02.021>.
- Barnes R, et al. Standard normal variate transformation and detrending of near-infrared diffuse reflectance spectra. *Appl Spectrosc*. 1989;43:772–7. <https://doi.org/10.1366/0003702894202201>.
- Bates D, et al. Package 'lme4': Convergence. 2015;12:2.
- Blanco M, Villarroya INIR. NIR spectroscopy: a rapid-response analytical tool. *TrAC Trends Anal Chem*. 2002;21:240–50. [https://doi.org/10.1016/S0165-9936\(02\)00404-1](https://doi.org/10.1016/S0165-9936(02)00404-1).
- Bokobza L. Origin of near-infrared absorption bands. Hoboken: Wiley; 2002. <https://doi.org/10.1002/9783527612666.ch02>.
- Bolster KL, et al. Determination of carbon fraction and nitrogen concentration in tree foliage by near infrared reflectances: a comparison of statistical methods. *Can J Forest Res*. 1996;26:590–600. <https://doi.org/10.1139/x26-068>.
- Borges DLG, Holcombe JA. Graphite furnace atomic absorption spectrometry. *Encyclopedia Anal Chem*. 2017. <https://doi.org/10.1002/9780470027318.a5108.pub3>.
- Caliori ÍP, et al. Estimation of cellulose crystallinity of sugarcane biomass using near infrared spectroscopy and multivariate analysis methods. *Carbohydr Polym*. 2017;158:20–8. <https://doi.org/10.1016/j.carbpol.2016.12.005>.
- Cánovas FM, et al. Nitrogen metabolism and biomass production in forest trees. *Front Plant Sci*. 2018;9:1449. <https://doi.org/10.3389/fpls.2018.01449>.
- Cooke JE, Weih M. Nitrogen storage and seasonal nitrogen cycling in *Populus*: bridging molecular physiology and ecophysiology. *New Phytol*. 2005;167:19–30. <https://doi.org/10.1111/j.1469-8137.2005.01451.x>.

12. Couture JJ, et al. Spectroscopic determination of ecologically relevant plant secondary metabolites. *Methods Ecol Evol.* 2016;7:1402–12. <https://doi.org/10.1111/2041-210X.12596>.
13. Croft H, Chen J. Leaf pigment content. Reference module in earth systems and environmental sciences. Oxford: Elsevier Inc; 2017. p. 1–22.
14. Curran PJ. Remote sensing of foliar chemistry. *Remote Sens Environ.* 1989;30:271–8. [https://doi.org/10.1016/0034-4257\(89\)90069-2](https://doi.org/10.1016/0034-4257(89)90069-2).
15. Cyr D, et al. Seasonal dynamics of carbohydrate and nitrogenous components in the roots of perennial weeds. *Plant Cell Environ.* 1990;13:359–65. <https://doi.org/10.1111/j.1365-3040.1990.tb02139.x>.
16. De Bei R, et al. Rapid measurement of total non-structural carbohydrate concentration in grapevine trunk and leaf tissues using near infrared spectroscopy. *Comput Electron Agric.* 2017;136:176–83. <https://doi.org/10.1016/j.compag.2017.03.007>.
17. Decruyenaere V, et al. Development of near-infrared spectroscopy calibrations to quantify starch and soluble sugar content in the roots of *Rumex obtusifolius*. *Weed Res.* 2012;52:1–5. <https://doi.org/10.1111/j.1365-3180.2011.00895.x>.
18. Eom S-H, et al. Far infrared ray irradiation stimulates antioxidant activity in *Vitis flexuosa* THUNB. berries. *Korean J Med Crop Sci.* 2007;15:319–23.
19. Evans JR. Nitrogen and photosynthesis in the flag leaf of wheat (*Triticum aestivum* L.). *Plant Physiol.* 1983;72:297–302. <https://doi.org/10.1104/pp.72.2.297>.
20. Famula RA, et al. Association genetics of carbon isotope discrimination and leaf morphology in a breeding population of *Juglans regia* L. *Tree Genet Genom.* 2019;15:6. <https://doi.org/10.1007/s11295-018-1307-4>.
21. Fernández JL, et al. Determination of the lignocellulosic components of olive tree pruning biomass by near infrared spectroscopy. *Energies.* 2019;12:2497. <https://doi.org/10.3390/en12132497>.
22. Forina M, et al. Iterative predictor weighting (IPW) PLS: a technique for the elimination of useless predictors in regression problems. *J Chemom.* 1999;13:165–84.
23. Forina M, et al. Artificial nose, NIR and UV–visible spectroscopy for the characterisation of the PDO Chianti Classico olive oil. *Talanta.* 2015;144:1070–8. <https://doi.org/10.1016/j.talanta.2015.07.067>.
24. García-Sánchez F, et al. 7 Irrigation and fertilization management in lime trees. The lime: botany, production and uses. Wallingfor: CAB; 2017. p. 91. <https://doi.org/10.1079/9781780647845.0091>.
25. Garriga M, et al. Chlorophyll, anthocyanin, and gas exchange changes assessed by spectroradiometry in *Fragaria chiloensis* under salt stress. *J Integr Plant Biol.* 2014;56:505–15.
26. Gebreselassie MN, et al. Near-infrared spectroscopy enables the genetic analysis of chemical properties in a large set of wood samples from *Populus nigra* (L.) natural populations. *Ind Crops Prod.* 2017;107:159–71. <https://doi.org/10.1016/j.indcrop.2017.05.013>.
27. Guillemain A, et al. Performance of NIR handheld spectrometers for the detection of counterfeit tablets. *Talanta.* 2017;165:632–40. <https://doi.org/10.1016/j.talanta.2016.12.063>.
28. Gundersen P. Nitrogen deposition and the forest nitrogen cycle: role of denitrification. *For Ecol Manage.* 1991;44:15–28. [https://doi.org/10.1016/0378-1127\(91\)90194-Z](https://doi.org/10.1016/0378-1127(91)90194-Z).
29. Gundersen P, et al. Impact of nitrogen deposition on nitrogen cycling in forests: a synthesis of NITREX data. *For Ecol Manage.* 1998;101:37–55. [https://doi.org/10.1016/S0378-1127\(97\)00124-2](https://doi.org/10.1016/S0378-1127(97)00124-2).
30. Han Q, Kabeya D. Recent developments in understanding mast seeding in relation to dynamics of carbon and nitrogen resources in temperate trees. *Ecol Res.* 2017;32:771–8. <https://doi.org/10.1007/s11284-017-1494-8>.
31. Hardin JA, et al. In situ measurement of pecan leaf nitrogen concentration using a chlorophyll meter and vis-near infrared multispectral camera. *HortScience.* 2012;47:955–60. <https://doi.org/10.21273/HORTSCI.47.7.955>.
32. Hu X-F, et al. The effects of simulated acid rain on internal nutrient cycling and the ratios of Mg, Al, Ca, N, and P in tea plants of a subtropical plantation. *Environ Monit Assess.* 2019;191:99. <https://doi.org/10.1007/s10661-019-7248-z>.
33. Huang J, Peng S. Comparison and standardization among chlorophyll meters in their readings on rice leaves. *Plant Prod Sci.* 2004;7:97–100. <https://doi.org/10.1626/pp.7.97>.
34. Inagaki T, et al. Determination of physical and chemical properties and degradation of archeological Japanese cypress wood from the Tohyamago area using near-infrared spectroscopy. *J Wood Sci.* 2018;64:347–55. <https://doi.org/10.1007/s10086-018-1718-8>.
35. Jiang AP, et al. Relationships of leaf color and pigment and nutrient elements in senescing leaves of *Sassafras tsumu*. *For Res.* 2016;29:362.
36. Jin X, et al. Determination of hemicellulose, cellulose and lignin content using visible and near infrared spectroscopy in *Miscanthus sinensis*. *Bioresour Technol.* 2017;241:603–9. <https://doi.org/10.1016/j.biortech.2017.05.047>.
37. Kokaly RF. Investigating a physical basis for spectroscopic estimates of leaf nitrogen concentration. *Remote Sens Environ.* 2001;75:153–61. [https://doi.org/10.1016/S0034-4257\(00\)00163-2](https://doi.org/10.1016/S0034-4257(00)00163-2).
38. Li G, Coleman GD. Nitrogen storage and cycling in trees. In: Advances in botanical research. New York: Elsevier; 2019. p. 127–55.
39. Li Y, Altaner C. Predicting extractives content of *Eucalyptus bosistoana* F. Muell. Heartwood from stem cores by near infrared spectroscopy. *Spectrochim Acta A Mol Biomol Spectrosc.* 2018;198:78–87. <https://doi.org/10.1016/j.saa.2018.02.068>.
40. Li Y, et al. Genetic variation in heartwood properties and growth traits of *Eucalyptus bosistoana*. *Eur J For Res.* 2018;137:565–72. <https://doi.org/10.1007/s10342-018-1125-0>.
41. Li Y, et al. Spectroscopic determination of leaf chlorophyll content and color for genetic selection on *Sassafras tsumu*. *Plant Methods.* 2019;15:73. <https://doi.org/10.1186/s13007-019-0458-0>.
42. Li Z, et al. Identification of oil, sugar and crude fiber during tobacco (*Nicotiana tabacum* L.) seed development based on near infrared spectroscopy. *Biomass Bioenergy.* 2018;111:39–45. <https://doi.org/10.1016/j.biombioe.2018.01.017>.
43. Liang L, et al. Prediction of holocellulose and lignin content of pulp wood feedstock using near infrared spectroscopy and variable selection. *Spectrochim Acta A Mol Biomol Spectrosc.* 2020;225:117515. <https://doi.org/10.1016/j.saa.2019.117515>.
44. Liu X, et al. Comparison of prediction power of three multivariate calibrations for estimation of leaf anthocyanin content with visible spectroscopy in *Prunus cerasifera*. *PeerJ.* 2019;7:e7997. <https://doi.org/10.7717/peerj.7997>.
45. Malagoli P, et al. Dynamics of nitrogen uptake and mobilization in field-grown winter oilseed rape (*Brassica napus*) from stem extension to harvest: I. Global N flows between vegetative and reproductive tissues in relation to leaf fall and their residual N. *Ann Bot.* 2005;95:853–61. <https://doi.org/10.1093/aob/mci091>.
46. Malegori C, et al. Comparing the analytical performances of Micro-NIR and FT-NIR spectrometers in the evaluation of acerola fruit quality, using PLS and SVM regression algorithms. *Talanta.* 2017;165:112–6. <https://doi.org/10.1016/j.talanta.2016.12.035>.
47. Mancini M, et al. Near infrared spectroscopy for the discrimination between different residues of the wood processing industry in the pellet sector. *Fuel.* 2018;217:650–5. <https://doi.org/10.1016/j.fuel.2018.01.008>.
48. Markwell J, et al. Calibration of the Minolta SPAD-502 leaf chlorophyll meter. *Photosynthesis Res.* 1995;46:467–72. <https://doi.org/10.1007/BF00032301>.
49. Mehmood T, et al. A review of variable selection methods in partial least squares regression. *Chemometr Intell Lab Syst.* 2012;118:62–9. <https://doi.org/10.1016/j.chemolab.2012.07.010>.
50. Mevik B et al. Partial least squares and principal component regression. R package version 2.5–0; 2015.
51. Millard P. Effect of nitrogen supply on growth and internal nitrogen cycling within deciduous trees. In: Annales des Sciences forestières. EDP Sciences: Les Ulis; 1989. p. 666–85.
52. Millard P. Ecophysiology of the internal cycling of nitrogen for tree growth. *J Plant Nutr Soil Sci.* 1996;159:1–10. <https://doi.org/10.1002/jpln.1996.3581590102>.
53. Millard P, Neilsen G. The influence of nitrogen supply on the uptake and remobilization of stored N for the seasonal growth of apple trees. *Ann Bot.* 1989;63:301–9. <https://doi.org/10.1093/oxfordjournals.aob.a087746>.
54. Millard P, Proe MF. Nitrogen uptake, partitioning and internal cycling in *Picea sitchensis* (Bong.) Carr. as influenced by nitrogen supply. *N Phytol.* 1993;125:113–9. <https://doi.org/10.1111/j.1469-8137.1993.tb03869.x>.
55. Min M, et al. Nondestructive detection of nitrogen in Chinese cabbage leaves using VIS–NIR spectroscopy. *HortScience.* 2006;41:162–6. <https://doi.org/10.21273/HORTSCI.41.1.162>.

56. Monje OA, Bugbee B. Inherent limitations of nondestructive chlorophyll meters: a comparison of two types of meters. *HortScience*. 1992;27:69–71 <https://doi.org/10.21273/HORTSCI.27.1.69>.
57. Moreau B et al. Estimating leaf nitrogen of eastern cottonwood trees with a chlorophyll meter. Gen Tech Rep SRS-71. US Department of Agriculture, Forest Service, Southern Research Station, Asheville, NC; 2004. p. 487–91.
58. Naing AH, et al. Overexpression of snapdragon *Delila* (*Del*) gene in tobacco enhances anthocyanin accumulation and abiotic stress tolerance. *BMC Plant Biol*. 2017;17:65. <https://doi.org/10.1186/s12870-017-1015-5>.
59. Nambiar EKS, Fife DN. Nutrient retranslocation in temperate conifers. *Tree Physiol*. 1991;9:185–207. <https://doi.org/10.1093/treephys/9.1-2.185>.
60. Padilla FM, et al. Evaluation of optical sensor measurements of canopy reflectance and of leaf flavonols and chlorophyll contents to assess crop nitrogen status of muskmelon. *Eur J Agron*. 2014;58:39–52. <https://doi.org/10.1016/j.eja.2014.04.006>.
61. Park S, et al. Rapid prediction of the chemical information of wood powder from softwood species using near-infrared spectroscopy. *BioResources*. 2018;13:2440–51. <https://doi.org/10.15376/biores.13.2.2440-2451>.
62. Paul V et al. Estimation of chlorophylls/photosynthetic pigments—their stability is an indicator of crop plant tolerance to abiotic stresses. In: Manual of ICAR sponsored training programme for technical staff of ICAR institutes on “physiological techniques to analyze the impact of climate change on crop plants”. 8; 2017.
63. Payne RJ, et al. Nitrogen deposition and plant biodiversity: past, present, and future. *Front Ecol Environ*. 2017;15:431–6. <https://doi.org/10.1002/fee.1528>.
64. Press WH, Teukolsky SA. Savitzky–Golay smoothing filters. *Comput Phys*. 1990;4:669–72. <https://doi.org/10.1063/1.4822961>.
65. Quentin AG, et al. Application of near-infrared spectroscopy for estimation of non-structural carbohydrates in foliar samples of *Eucalyptus globulus* Labillardière. *Tree Physiol*. 2017;37:131–41.
66. R Core Team. R: A Language and Environment for Statistical Computing. Vienna: R Foundation for Statistical Computing; 2017.
67. Ramirez JA, et al. Near-infrared spectroscopy (NIRS) predicts non-structural carbohydrate concentrations in different tissue types of a broad range of tree species. *Methods Ecol Evol*. 2015;6:1018–25. <https://doi.org/10.1111/2041-210X.12391>.
68. Rivero-Villar A, et al. Differences in nitrogen cycling between tropical dry forests with contrasting precipitation revealed by stable isotopes of nitrogen in plants and soils. *Biotropica*. 2018;50:859–67. <https://doi.org/10.1111/btp.12612>.
69. Robinson KM, et al. Genetic variation in functional traits influences arthropod community composition in aspen (*Populus tremula* L.). *PLoS ONE*. 2012. <https://doi.org/10.1371/journal.pone.0037679>.
70. Schneider S, et al. Soluble N compounds in trees exposed to high loads of N: a comparison of spruce (*Picea abies*) and beech (*Fagus sylvatica*) grown under field conditions. *N Phytol*. 1996;134:103–14. <https://doi.org/10.1111/j.1469-8137.1996.tb01150.x>.
71. Shi J-Y, et al. Determination of total flavonoids content in fresh Ginkgo biloba leaf with different colors using near infrared spectroscopy. *Spectrochim Acta A Mol Biomol Spectrosc*. 2012;94:271–6. <https://doi.org/10.1016/j.saa.2012.03.078>.
72. Siesler HW, et al. Near-infrared spectroscopy: principles, instruments, applications. Hoboken: John Wiley & Sons; 2008. <https://doi.org/10.1002/9783527612666>.
73. Sinclair T, Horie T. Leaf nitrogen, photosynthesis, and crop radiation use efficiency: a review. *Crop Sci*. 1989;29:90–8. <https://doi.org/10.2135/cropsci1989.0011183X002900010023x>.
74. Srinivasan A. Handbook of precision agriculture: principles and applications. Boca Raton: CRC Press; 2006. <https://doi.org/10.1201/9781482277968>.
75. Stevens A, Ramirez-Lopez L. An introduction to the prospectr package. R Package Vignette, Report No.: R Package Version 0.1 3; 2014.
76. Strack D, Wray V. Anthocyanins. In: *Methods in plant biochemistry*. New York: Elsevier; 1989. p. 325–56.
77. Sui YH, et al. Inheritance of anthocyanin contents in leaves of chili pepper. *J Nanjing Univ Nat Sci*. 2009;32(3):19–24.
78. Swarts N. Precision fertigation for improved apple orchard productivity. In: 2016 future orchards national tour; 2016. p. 1–25.
79. Tran TN, et al. Interpretation of variable importance in partial least squares with significance multivariate correlation (sMC). *Chemometr Intell Lab Syst*. 2014;138:153–60. <https://doi.org/10.1016/j.chemolab.2014.08.005>.
80. Tremblay N, et al. Sensing crop nitrogen status with fluorescence indicators A review. *Agron Sustain Dev*. 2012;32:451–64. <https://doi.org/10.1007/s13593-011-0041-1>.
81. Trojak M, Skowron E. Role of anthocyanins in high-light stress response. *World Sci News*. 2017;81:150–68.
82. Villar-Salvador P, et al. The role of stored carbohydrates and nitrogen in the growth and stress tolerance of planted forest trees. *New For*. 2015;46:813–39. <https://doi.org/10.1007/s11056-015-9499-z>.
83. Wellburn AR. The spectral determination of chlorophylls a and b, as well as total carotenoids, using various solvents with spectrophotometers of different resolution. *J Plant Physiol*. 1994;144:307–13. [https://doi.org/10.1016/S0176-1617\(11\)81192-2](https://doi.org/10.1016/S0176-1617(11)81192-2).
84. Wickham H. ggplot2: elegant graphics for data analysis. Berlin: Springer; 2016.
85. Wijewardane NK, et al. Moisture insensitive prediction of soil properties from VNIR reflectance spectra based on external parameter orthogonalization. *Geoderma*. 2016;267:92–101. <https://doi.org/10.1016/j.geoderma.2015.12.014>.
86. Wold S, et al. PLS-regression: a basic tool of chemometrics. *Chemometr Intell Lab Syst*. 2001;58:109–30. [https://doi.org/10.1016/S0169-7439\(01\)00155-1](https://doi.org/10.1016/S0169-7439(01)00155-1).
87. Wood C et al. Relationships between chlorophyll meter readings and leaf chlorophyll concentration, N status, and crop yield: a review. In: *Proceedings of the agronomy society of New Zealand*; 1993, pp. 1–9.
88. Workman J Jr, Weyer L. Practical guide and spectral atlas for interpretive near-infrared spectroscopy. Boca Raton: CRC Press; 2012. <https://doi.org/10.1201/b11894>.
89. Yang S, et al. Classification of the hot air heat treatment degree of larch wood using a multivariate analysis of near-infrared spectroscopy. *J Wood Sci*. 2018;64:220–5. <https://doi.org/10.1007/s10086-018-1706-z>.
90. Zhang Y, et al. The contents of terpene trilactone and flavonoid in leaves of seedlings from ancient female *Ginkgo* trees in China. *Hortic Plant J*. 2017;3:165–71. <https://doi.org/10.1016/j.hpj.2017.06.002>.
91. Zhao P, Cao J. Wood species identification using spectral reflectance feature and optimal illumination radian design. *J For Res*. 2016;27:219–24. <https://doi.org/10.1007/s11676-015-0171-4>.

Publisher's Note

Springer Nature remains neutral with regard to jurisdictional claims in published maps and institutional affiliations.